JOURNAL OF SYNCHROTRON RADIATION

ISSN 1600-5775

Phase-space matching between bent Laue and flat Bragg crystals

Z. Zhong,[a]* M. Hasnah,[b] A. Broadbent,[a] E. Dooryhee[a] and M. Lucas[a]

[a]National Syncrhrotron Light Source II, Brookhaven National Laboratory, Upton, NY 11973, USA, and [b]Department of Mathematics, Statistics and Physics, Qatar University, Al Jamiaa Street, Doha, Qatar. *Correspondence e-mail: zhong@bnl.gov

Received 28 May 2019
Accepted 1 August 2019

Edited by A. Momose, Tohoku University, Japan

Keywords: bent Laue crystals; Dumond diagram; phase-contrast imaging; analyser-based imaging; diffraction-enhanced imaging; monochromator; analyzers; phase space; high-energy X-rays.

Through phase-space analysis of Dumond diagrams for a flat Bragg crystal, a single bent Laue crystal and a monochromator consisting of double-bent Laue crystals, this work shows that it is possible to match the flat Bragg crystal to both the single-crystal and double-crystal Laue monochromators. The matched system has the advantage that the phase space of the bent crystal's output beam is much larger than that of the flat crystal, making the combined system stable. Here it is suggested that such a matched system can be used at synchrotron facilities to realize X-ray dark-field imaging, analyzer-based imaging and diffraction-enhanced imaging at beamlines using double-Laue monochromators.

1. Introduction

Flat Bragg crystals have been extensively used at synchrotron beamlines as monochromators. A monochromator consisting of two parallel crystals (dual-crystal) is necessary to bring the output monochromatic beam parallel to the storage ring floor and to keep the output beam at the same location when the energy is tuned. Ideally, both crystals should have exactly the same temperature and heat load to enable phase-space matching between the two flat crystals. However, due to the large heat load on the first crystal, such matching is difficult (Lee *et al.*, 2000; Zhong *et al.*, 2000), and with the advancement of more powerful insertion devices the heat-load problem becomes worse. Cryogenic cooling, an expensive technique, must be employed at most synchrotron beamlines nowadays. However, even cryogenic cooling is having limited success at some beamlines (Lee *et al.*, 2000). Instead of crystal cryogenic cooling, bent Laue crystals have been used at many high-energy X-ray beamlines partly due to the smaller heat load of the Laue crystal – most of the filtered beam power transmits through the crystal instead of being absorbed, whereas a Bragg crystal absorbs all the power in the beam. Bent Laue crystals also have the advantage of larger and tunable bandwidth. It would be ideal to develop a system that employs a bent Laue crystal as the first crystal to solve the heat-load problem as well as a traditional flat Bragg crystal as the second crystal. Conventional wisdom suggests that the matching of a Bragg crystal with a bent Laue crystal would be impossible, and thus has never been utilized. Here we show, through analysis of phase space, that it is indeed possible to match the different crystals. Furthermore, the matched system has the advantage that the first crystal's output beam's phase space is much larger than that of the second crystal, making the combined system more stable than the traditional Bragg–Bragg arrangement.

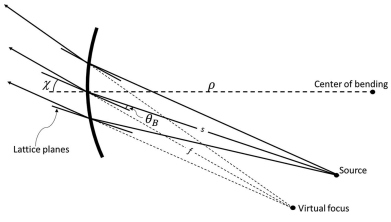

Practically, many synchrotron imaging beamlines use bent Laue double-crystal monochromators to produce high-flux beams with a large energy bandwidth. Examples include the BMIT beamline at the Canadian Light Source (Wysokinski *et al.*, 2016), the JEEP ID12 beamline at Diamond Light Source, UK (Drakopoulos *et al.*, 2015) and The Biomedical Beamline ID-17 of the European Synchrotron Radiation Facility (Diemoz *et al.*, 2010; Zhao *et al.*, 2012). The HEX (high-energy engineering X-ray scattering) beamline, being designed for the NSLS-II, will also use a double-bent Laue–Laue monochromator. The capability of these beamlines would be greatly enhanced if phase-contrast methods such as X-ray dark-field imaging (XDFI) (Ando *et al.*, 2016), analyzer-based imaging (ABI) (Bravin *et al.*, 2013) or diffraction-enhanced imaging (DEI) can be employed using an existing monochromator. These phase-contrast methods all depend on the small intrinsic rocking curve width of high-index reflection of perfect flat Bragg crystals. We will use DEI from this point on for simplicity, but the conclusions apply equally well to XDFI and ABI. With the phase-space method we develop here, we show that DEI can indeed be implemented with ease at beamlines with bent Laue monochromators.

2. Phase space of a perfect flat crystal

The phase space of a perfect flat crystal is well understood and is best depicted with a Dumond diagram. Fig. 1 shows the Dumond diagram of the 111 reflection, typically used by monochromators for diffraction and spectroscopy, and of the 333 reflection, typically used for DEI due to its much narrower rocking-curve width. Using analytical formulas based on dynamical theory of X-ray diffraction, a software code was written using IDL programming language to simulate and display the Dumond diagram. We assume an angular divergence of 200 µrad, typical at modern synchrotron facilities (Suortti *et al.*, 2000). This diagram assumes that collimating mirrors are not used. An X-ray energy of 30 keV is assumed.

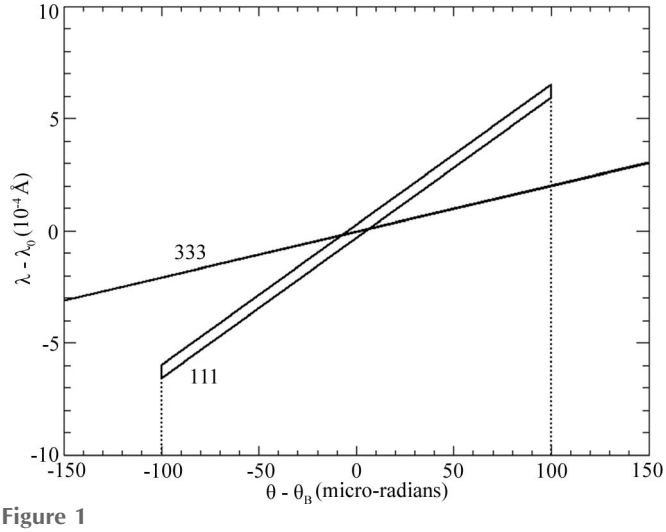

Figure 1
Dumond diagram of a two-crystal system consisting of a perfect crystal with 111 reflection and a perfect crystal with 333 reflection.

It is seen that the vertical divergence of the beam dominates the bandwidth of the output beam. The intrinsic Darwin width is smaller in comparison, especially for the 333 reflection. For each phase space, the horizontal width is the Darwin width. The slope is $2d\cos(\theta)$, where d is the d-spacing of the reflection. We note that there is little overlap, about 15 µrad, between the 111 and 333 reflections. This means that if one attempts to perform XDFI, ABI or DEI with the 333 reflection at a typical beamline with a 111 monochromator, the beam for phase-contrast imaging will only be 15 µrad in divergence compared with the 200 µrad divergence of the incident beam, thus more than 90% of the beam will be lost. This highlights the importance of matching crystals in phase space.

3. Phase space of a bent Laue crystal

Phase space of bent Laue crystals involves consideration of the bent crystal's modification of divergence and the larger bandwidth of the output beam. Fig. 2 is a schematic diagram of a bent Laue crystal reflecting a diverging beam, where the crystal is assumed to be cylindrically bent. The X-ray incident beam from the point source is diffracted by the bent Laue crystal. The plane of diffraction is in the figure plane. The diffracted beam is focused at a virtual focal point.

The angle between the normal to the crystal surface and the lattice planes used for diffraction is called $\chi\theta_B$ (the Bragg angle) and is defined as the angle between an incident X-ray beam and a set of crystal lattice planes used for diffraction. The distance from the point source to the center of the crystal is s and the distance from the virtual focus to the center of the crystal is f. For the case in Fig. 2, f is negative since it is virtual. The relationship between s and f can be expressed as

$$\frac{2}{\rho} = \frac{\cos(\chi \mp \theta_B)}{s} - \frac{\cos(\chi \pm \theta_B)}{f}, \qquad (1)$$

where ρ is the bending radius of the bent crystal. ρ is positive when the source point is on the concave side of the crystal (as in Fig. 2) and negative with the source on the convex side (Zhong *et al.*, 2001). The upper sign corresponds to when the source and the center of bending are on the same side of the crystal's lattice plane (as shown in Fig. 2). For the lower sign, the source and the center of bending are on different sides of

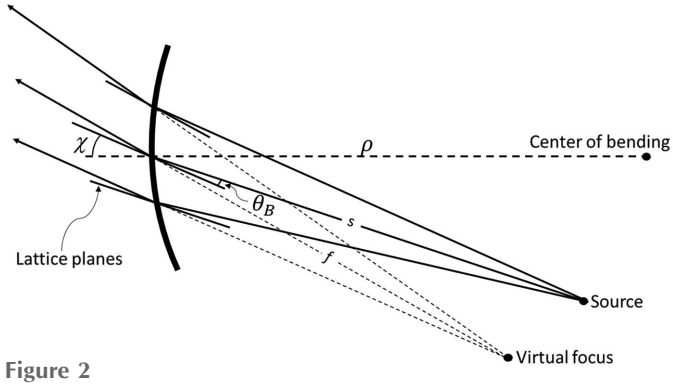

Figure 2
Geometrical optics considerations for a cylindrically bent Laue crystal.

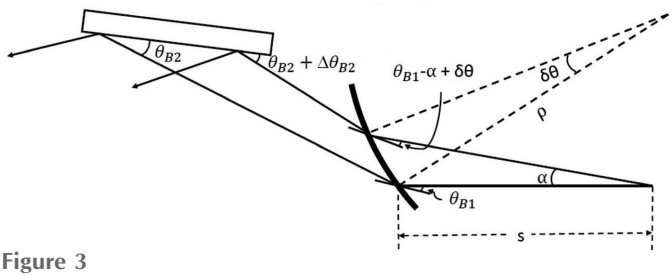

Figure 3
Schematic representation of a two-crystal system consisting of a cylindrically bent Laue first crystal and a flat Bragg second crystal. The diffraction orders and Bragg angles of the crystals can be different.

the lattice plane. We will assume the upper sign case herein (*i.e.* the source and center of bending are on the same side of the lattice planes).

In order to produce the highest monochromaticity, the variation of the angle of incidence along the crystal surface must be zero ($\Delta\theta = 0$). Such condition is achieved when

$$s = \rho\cos(\chi - \theta_{\rm B}) \tag{2}$$

and

$$f = -\rho\cos(\chi + \theta_{\rm B}). \tag{3}$$

In this special case, commonly referred to as the inverse Cauchois geometry, both the source and the focal point are on the Rowland circle, which is a circle whose diameter equals the bending radius of the crystal.

Fig. 3 shows the beam diffracted by a single bent Laue monochromator striking a flat Bragg crystal. It shows that the rays incident upon and diffracted by the bent Laue crystal have different angles and consequently different wavelengths. The angle–wavelength association (phase space) of the diffracted beam that then strikes the flat Bragg crystal is normally not matched to that of the Bragg crystal. Analysis of the variation of the angle of incidence on the Bragg crystal lattice planes is necessary to find the condition under which the phase spaces match.

The Laue and Bragg crystals have lattice spacings of d_1 and d_2 with corresponding Bragg angles $\theta_{\rm B1}$ and $\theta_{\rm B2}$, respectively. In Fig. 3, α is the divergence from the central ray of an arbitrary X-ray striking the bent Laue crystal. This X-ray strikes the bent Laue crystal at a different location to the center ray. Since the crystal is bent, the lattice planes at the location are tilted by $\delta\theta$ relative to the planes struck by the center ray,

$$\delta\theta = \frac{s\alpha}{\rho\cos(\chi - \theta_{\rm B1})}. \tag{4}$$

Assuming that the center ray makes $\theta_{\rm B}$ with the lattice planes, the incident angle of the X-ray is $\theta_{\rm B1} - \alpha + \delta\theta$. The deviation of the incident angle ($\Delta\theta_{\rm B1}$) from $\theta_{\rm B1}$ is then

$$\Delta\theta_{\rm B1} = -(\alpha - \delta\theta) = \alpha\left[\frac{s}{\rho\cos(\chi - \theta_{\rm B1})} - 1\right]. \tag{5}$$

The lattice spacing for a bent Laue crystal changes from the front to the back face of the crystal, thus d_1 denotes the average lattice spacing of bent Laue crystal diffraction. The side of the crystal closer to the center of bending is under compressive strain and the other side is under tensile strain. This effect contributes to a larger bandwidth of the bent Laue crystal compared with a perfect crystal. The average lattice spacing across the thickness is the same as that of a perfect crystal. According to Bragg's law, $\lambda_1 = 2d_1\sin\theta_{\rm B1}$; the deviation of the wavelength, $\Delta\lambda_1$, from that of the wavelength of the center ray is

$$\Delta\lambda_1 = 2\Delta\theta_{\rm B1}d_1\cos\theta_{\rm B1}. \tag{6}$$

The deviation of the angle of the diffracted beam from the nominal $2\theta_{\rm B1}$ is

$$\Delta\varphi = 2\Delta\theta_{\rm B1}. \tag{7}$$

Assuming that the Bragg crystal is set so that its lattice planes make the correct Bragg angle ($\theta_{\rm B2}$) with the center ray of the beam diffracted by the Laue crystal, it is seen from Fig. 3 that the deviation $\Delta\theta_{\rm B2}$ of the incident angle from the Bragg angle $\theta_{\rm B2}$ is

$$\Delta\theta_{\rm B2} = 2\Delta\theta_{\rm B1} + \alpha = \alpha\left[\frac{2s}{\rho\cos(\chi - \theta_{\rm B1})} - 1\right]. \tag{8}$$

Assuming that the Bragg crystal diffracts the incident X-ray beam, then the deviation of the wavelength from the center ray wavelength is $\Delta\lambda_2$. According to Bragg's law,

$$\Delta\lambda_2 = 2\Delta\theta_{\rm B2}d_2\cos\theta_{\rm B2}. \tag{9}$$

Since $\Delta\lambda_1$ and $\Delta\lambda_2$ concern the same X-ray beam, requiring these to be equal results in the condition under which the phase spaces of the crystals are matched. Thus the condition is

$$d_2\cos\theta_{\rm B2}\left[\frac{2s}{\rho\cos(\chi-\theta_{\rm B1})} - 1\right] = d_1\cos\theta_{\rm B1}\left[\frac{s}{\rho\cos(\chi-\theta_{\rm B1})} - 1\right]. \tag{10}$$

The required bending radius of the Laue crystal for achieving matching of the phase space can then be solved for each known asymmetry angle, lattice spacing d_1 and d_2 and source-to-crystal distance,

$$\rho = s\frac{2d_2\cos\theta_{\rm B2} - d_1\cos\theta_{\rm B1}}{\cos(\chi - \theta_{\rm B1})(d_2\cos\theta_{\rm B2} - d_1\cos\theta_{\rm B1})}. \tag{11}$$

Consider the special case where both crystals use the same reflection, the condition above gives ρ as infinity. This is the well known +− (non-dispersive) condition (Authier, 2012; Guigay *et al.*, 2013) for perfect, un-bent crystals. Thus it is impossible to match a bent Laue with a flat Bragg crystal when both crystals use the same reflection. This confirms the intuitive assessment made in the *Introduction*.

Now consider a special case where the bent Laue crystal uses the 111 reflection of silicon, and the perfect Bragg crystal uses the 333 reflection. In this case, $d_1 = 3d_2$. Using the simplification that at high X-ray energies $\cos\theta_{\rm B}$ is approximately unity, we have the condition for matching of phase space in this unique case,

$$\rho = \frac{s}{2\cos(\chi - \theta_{\rm B1})}. \tag{12}$$

Comparing equation (2) with equation (12) shows that, in this special case, the Laue crystal needs to be bent to – interestingly – exactly half the radius required for inverse Cauchois geometry to allow phase-space matching.

To implement this condition practically, one can construct a Laue–Bragg monochromator, with the second crystal being a Bragg crystal using 333 reflection, and bend the first crystal to the radius specified in equation (12). This results in a monochromator suitable for delivering a beam for DEI. To achieve DEI, a Bragg 333 crystal analyzer is placed behind the Bragg crystal shown in Fig. 3. Note that, since the 333 reflection has a much larger Bragg angle than the 111 reflection, the monochromatic output beam will be at an angle relative to the incident white beam. This requires a small distance between the monochromator and the analyzer to be practical.

To gain intuition into the above analysis, Dumond diagrams were used to illustrate matching and non-matching conditions for a few special cases. A software code was written using IDL programming language to simulate and display the Dumond diagram. The code takes input from the lamellar model (Erola *et al.*, 1990) to simulate the bandwidth of the diffracted beam by the bent Laue crystal. The proposed HEX monochromator parameters (thickness = 2 mm, asymmetry angle = 35.3°) are used for generating the diagram. Note that 35.3° corresponds to the angle between a 100 crystal surface and a 111 reflection in a Laue crystal. ρ_c is defined as $s/\cos(\chi - \theta_{B1})$ – the bending radius of the inverse Cauchois geometry. Fig. 4 shows the Dumond diagrams of a bent crystal using 111 reflection with bending radii of $0.375\rho_c$, $\rho_c/2$, ρ_c, $2\rho_c$ and infinity (un-bent perfect crystal). The relative divergence (horizontal axis) and wavelength (vertical axis) changes shown in Fig. 4 are from the perspective of the Bragg 333 crystal. We assume 30 keV X-ray energy. The 333 flat crystal phase space is also shown. At a source distance (s) of 32 m, a bending radius of 37.5 m corresponds to the inverse Cauchois geometry.

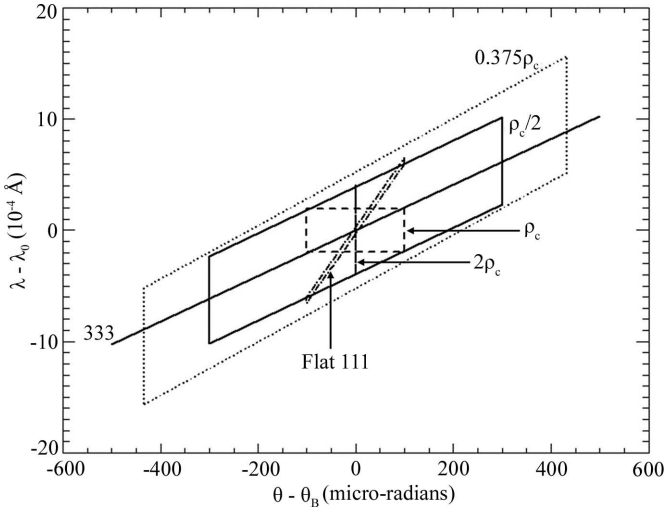

Figure 4
Dumond diagram for the two-crystal system shown in Fig. 3, with the first crystal bent to representative radii of $0.375\rho_c$, $\rho_c/2$, ρ_c $2\rho_c$ and infinity. A bending radius of infinity (flat 111) corresponds to a perfect crystal.

It is observed that, as the bending radius changes, the widths and slopes of the output beam phase spaces change character. For example, the slope can change from positive (for an unbent crystal) to 0 (at $\rho = \rho_c$). Compared with the difficulty of matching flat 111 and 333 crystals due to their different slopes, here with the ability to adjust the bending radius it would be possible to perfectly match the phase space of a bent Laue crystal with 111 reflection with that of a flat 333 reflection.

At $\rho = \rho_c$, as predicted by the inverse Cauchois geometry, the output beam of the bent Laue crystal has the same wavelength regardless of the divergence. This explains the rectangular shape of the phase space. The vertical height of the rectangle corresponds to the large bandwidth of the monochromatic beam due to the crystal being bent. This gives us confidence that the program generating the Dumond diagram is correct.

The vertical line corresponding to $\rho = 2\rho_c$ means that in this case the output beam is a parallel beam with a divergence of 0. When the bending is twice what is required for inverse Cauchois geometry, a bent Laue crystal outputs a parallel beam, as derived theoretically and proven experimentally by Zhong *et al.* (2001). This special case again validates the Dumond diagram.

We note that due to the much larger bandwidth (vertical height in the diagram) of the bent crystal, a monochromator constructed of a bent-Laue/flat-Bragg crystal is more stable. We also note that, while the bent crystal modifies the divergence of the beam, the flat 333 crystal perfectly accepts the beam with much larger divergence for cases when the bending radius of the first crystal is either $\rho_c/2$ or $0.375\rho_c$ (the divergence is expanded by a factor of 3 for $\rho = \rho_c/2$, and a factor of 4.3 for $\rho = 0.375\rho_c$). At these bending radii, the two-crystal system essentially acts as a beam expander. Beam expansion is typically achieved with much difficulty via asymmetric Bragg crystals, with limited energy-tunability. Thus, a dual-crystal monochromator using a bent Laue and a flat Bragg crystal has the potential to be a viable alternative beam expander providing a uniform beam with better energy tunability.

4. Double Laue–Laue phase space

A double Laue monochromator employs two crystals bent in the same direction at approximately the same bending radius. Unlike single bent Laue crystals discussed previously, the double-crystal monochromator does not modify the divergence of the beam. This is because the modification made by the first crystal is canceled by the second one reflecting the opposite way.

Both crystals are typically bent towards the source to minimize energy difference between top and bottom parts of the beam. As noted previously, replacing the second crystal with a perfect Bragg crystal allows phase-space matching, but has the undesirable effect that the output beam is not parallel to the incident beam. For performing DEI experiments, it is more desirable to deliver the double-bent Laue beam into the experimental hutch and then use a 333 perfect Bragg crystal as a post-monochromator. Here we derive the condition for

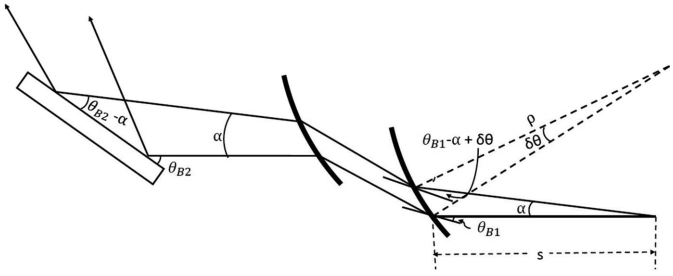

Figure 5
Schematic representation of a phase-contrast imaging system consisting of a double-bent Laue monochromator and a flat Bragg crystal.

phase-space matching a double-crystal Laue monochromator with a perfect Bragg flat crystal.

As with the single Laue crystal case, the wavelength of the beam at angle α relative to the central ray is defined by the source-to-crystal distance, asymmetry angle and the bending radius according to equation (6). The output beam maintains the same divergence as the incident beam for the double-crystal monochromator. Thus, assuming that the Bragg crystal is set so that its lattice planes make the correct Bragg angle (θ_{B2}) with the center ray of the monochromatic beam produced by the double-Laue monochromator, Fig. 5 shows that in this case the deviation $\Delta\theta_{B2}$ of the incident angle from the Bragg angle θ_{B2} is simply

$$\Delta\theta_{B2} = -\alpha. \tag{13}$$

Again, assuming that the Bragg crystal diffracts the beam, the deviation of the wavelength from the center ray wavelength $\Delta\lambda_2$ is

$$\Delta\lambda_2 = -2\alpha d_2 \cos\theta_{B2}. \tag{14}$$

Requiring $\Delta\lambda_1$ in equation (6) to be the same as $\Delta\lambda_2$ results in a bending radius that allows the phase space of the Bragg pre-monochromator to match that of the double-Laue monochromator,

$$\rho = s\frac{d_1\cos\theta_{B1}}{\cos(\chi-\theta_{B1})(d_1\cos\theta_{B1} - d_2\cos\theta_{B2})}. \tag{15}$$

For the special case where both crystals use the same reflection, the condition above requires that ρ is infinity, meaning that the Laue crystals are un-bent. This is the well known +−+ (non-dispersive) condition (Authier, 2012; Guigay *et al.*, 2013) for perfect, un-bent Bragg crystals. The analysis above confirms that the same condition holds true when two of the three crystals are Laue crystals.

Now consider the special case where the first two bent Laue crystals use the 111 reflection of silicon and the perfect Bragg crystal uses the 333 reflection. This situation is realistic since many high-energy X-ray imaging beamlines (BMIT at the Canadian Light Source, IMBL at the Australian Light Source, JEEP at the Diamond Light Source in UK and the Biomedical Beamline at the ESRF) use a 111 bent Laue crystal, whereas many DEI experiments (Chapman *et al.*, 1997; Dilmanian *et al.*, 2000; Rigon *et al.*, 2008; Zhao *et al.*, 2012) use a 333 perfect Bragg crystal. In particular, the ABI setup at the Biomedical

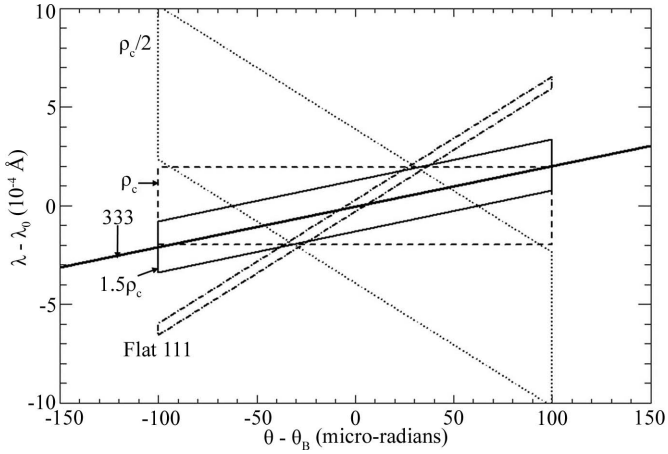

Figure 6
Dumond diagram for the bent Laue monochromator and analyzer system shown in Fig. 5, with the monochromator crystals being flat and bent to representative radii of $0.5\rho_c$, ρ_c and $1.5\rho_c$.

Beamline of ESRF is based on a double-Laue monochromator with 111 pre-monochromator followed by a flat Bragg 333 monochromator/analyzer. In this case, $d_1 = 3d_2$, we have the condition for matching of phase space in this unique case,

$$\rho = \frac{3s}{2\cos(\chi-\theta_{B1})}. \tag{16}$$

Comparison of equation (2) with equation (16) shows that in this special case the Laue crystal needs to be bent to 1.5 times the radius required for inverse Cauchois geometry to allow phase-space matching.

To gain intuition into the above analysis, Dumond diagrams were used to illustrate matching. Fig. 6 shows the Dumond diagrams of the phase space of the output beam from a double-crystal bent Laue monochromator at 30 keV. Both crystals are assumed to be using 111 reflection bent to $\rho_c/2$, ρ_c, $3/2\rho_c$, $2\rho_c$ and infinity (un-bent perfect crystal). The 333 flat crystal phase space is also shown. The proposed HEX monochromator parameters (thickness = 2 mm, asymmetry angle = 35.3°, source-to-monochromator distance s = 32 m) are used for generating the diagram.

Fig. 6 shows that, at 56.3 m bending radius, when ρ is $3/2\rho_c$, with both crystals bent towards the source, there is perfect matching between the phase space of a 333 perfect crystal and the double-crystal bent Laue–Laue monochromator. It is seen that the output beam of the 333 Bragg crystal has a divergence of 200 µrad, which is the same as that of the beam produced by the double-Laue monochromator. This divergence is large compared with the Darwin width of the 333 reflection at 1.9 µrad. To perform DEI in this system, one needs to place a 333 Bragg crystal analyzer behind the 333 Bragg crystal (shown in Fig. 5) in a +− arrangement and position the sample between the two Bragg crystals. Despite the large divergence of the incident beam, the rocking curve of the analyzer crystal will be triangular with a narrow full width at half-maximum (FWHM) of approximately 1.9 µrad. The idea of realizing a narrow rocking curve, which enables DEI, with a pair of 333

crystals in a beam with much larger divergence is illustrated and experimentally proven by Zhong *et al.* (2001).

Using the lamellar model (Erola *et al.*, 1990), the FWHM for the bent Laue crystal reflection is 42 μrad. This suggests that DEI can be implemented at imaging beamlines using double-bent Laue monochromators with excellent intensity stability.

As with the Laue/Bragg case shown above, it is seen that in the double-Laue/Bragg system, as the bending radius changes, the width and slope of the output beam phase space change character. The slope can change from negative (for $\rho = \rho_c/2$) to 0 (at $\rho = \rho_c$) and progressing to positive as the crystal is bent less (larger ρ) towards the source. We again note that, due to the much larger bandwidth (vertical height in the diagram) of the bent crystal, a system constructed of bent double-Laue/flat Bragg crystals is more stable. Unlike the Laue/Bragg case, the double-Laue/Bragg system has the advantage that it does not modify the divergence of the beam.

5. Discussion

The Dumond diagrams shown above all assume an X-ray energy of 30 keV. One advantage of synchrotron radiation is energy tunability. It would be desirable to maintain phase-space matching when energy is tuned without changing the bending radius. At the high X-ray energies concerned, the Bragg angle θ_{B1} is small, making $2\cos(\chi - \theta_{B1})$ approximately independent of small changes in the Bragg angle. Applying this approximation, equations (12) and (16) show that indeed the bending radius does not need to change when the energy is changed.

The reflectivity of a perfect flat crystal is close to 100%. The reflectivity of a bent Laue crystal depends on X-ray energy, bending radius and asymmetry angle. We need to ensure that, at matching conditions, the reflectivity of bent Laue crystal is acceptable. Simulation using the lamellar model for the case where the double-crystal Laue monochromator matches Bragg 333 shows that the reflectivity is about 60%.

Until now it was thought that the non-dispersive condition with perfect phase-space matching was only possible with two reflections of exactly the same d-spacing. Typically the phase space is given by the nature of the reflection chosen, with limited ability to manipulate to suit the optical needs. We show that by using bent Laue optics one can achieve non-dispersive conditions for reflections of different reflection indices. Since the derivations above depend only on the d-spacing, perfect phase spacing is possible between silicon and diamond crystals. Furthermore, we introduced the concept of manipulating the phase space via adjusting the bending radius of a bent Laue crystal. In addition to making it possible to perform XDFI, ABI or DEI with high-index 333 reflection at a beamline equipped with a typical bent Laue monochromator using low-index reflection 111 (in this case, the 333 Bragg crystal is a pre-monochromator), we believe this new concept of phase-space manipulation could have profound implications for other areas of research involving X-rays such as construction of a novel beam expanding monochromator via combining a bent Laue crystal and a higher index Bragg crystal.

6. Conclusions

Analysis of the variation of angle and wavelength phase space was performed for a system consisting of a single bent Laue crystal and flat Bragg crystal, and a system consisting of a monochromator with double-bent Laue crystals and a flat Bragg crystal. In both cases it was shown that it is possible to match the flat Bragg crystal to the bent Laue crystals of different reflections, thus realizing a perfect phase-space match between different reflections. Dumond diagrams for a flat Bragg crystal and the two bent Laue crystal systems were created to illustrate the concept of phase-space manipulation by adjusting the bending radius. Furthermore, the Dumond diagrams show that the matched system has the advantage that the phase space of bent crystal's output beam is much larger than that of the flat crystal, making the combined system stable. We prove that such a matched system can be used at synchrotron facilities to realize, for example, diffraction-enhanced imaging at beamlines using double-Laue monochromators.

Acknowledgements

We are grateful to Milinda Abeykoon, Jianming Bai, Lonny Berman, Dean Chapman, Michael Drakopoulos, Daniel Fischer, Sanjit Ghose, Daniel Hausermann, Steven Hulbert, Cherno Jaye, Gihan Kwon, Wah-Keat Lee, Daniel Olds, Bruce Ravel, Qun Shen, Xianbo Shi, Peter Siddons, William Thomlinson, Ke Yang, Conan Weiland, Joseph Woicik and Tomasz Wysokinski for helpful discussions about this work. We would like to thank Jennifer Zhong for proof-reading the manuscript.

Funding information

This work is supported by the National Synchrotron Light Source II, a US DOE Office of Science User Facility operated for the DOE Office of Science by Brookhaven National Laboratory (contract No. DE-SC0012704 awarded to ZZ, AB, ED and ML) and by the Qatar University (grant No. QUUG-CAS-DMSP-2017-1 awarded to MH).

References

Ando, M., Sunaguchi, N., Shimao, D., Pan, A., Yuasa, T., Mori, K., Suzuki, Y., Jin, G., Kim, J. K., Lim, J. H., Seo, S. J., Ichihara, S., Ohura, N. & Gupta, R. (2016). *Phys. Med.* **32**, 1801–1812.
Authier, A. (2012). *Acta Cryst.* A**68**, 40–56.
Bravin, A., Coan, P. & Suortti, P. (2013). *Phys. Med. Biol.* **58**, R1–R35.
Chapman, D., Thomlinson, W., Johnston, R. E., Washburn, D., Pisano, E., Gmür, N., Zhong, Z., Menk, R., Arfelli, F. & Sayers, D. (1997). *Phys. Med. Biol.* **42**, 2015–2025.
Diemoz, P. C., Coan, P., Glaser, C. & Bravin, A. (2010). *Opt. Express*, **18**, 3494–3509.
Dilmanian, F. A., Zhong, Z., Ren, B., Wu, X. Y., Chapman, L. D., Orion, I. & Thomlinson, W. C. (2000). *Phys. Med. Biol.* **45**, 933–946.
Drakopoulos, M., Connolley, T., Reinhard, C., Atwood, R., Magdysyuk, O., Vo, N., Hart, M., Connor, L., Humphreys, B.,

Howell, G., Davies, S., Hill, T., Wilkin, G., Pedersen, U., Foster, A., De Maio, N., Basham, M., Yuan, F. & Wanelik, K. (2015). *J. Synchrotron Rad.* **22**, 828–838.
Erola, E., Eteläniemi, V., Suortti, P., Pattison, P. & Thomlinson, W. (1990). *J. Appl. Cryst.* **23**, 35–42.
Guigay, J.-P., Ferrero, C., Bhattacharyya, D., Mathon, O. & Pascarelli, S. (2013). *Acta Cryst.* A**69**, 91–97.
Lee, W.-K., Fernandez, P. & Mills, D. M. (2000). *J. Synchrotron Rad.* **7**, 12–17.
Rigon, L., Astolfo, A., Arfelli, F. & Menk, R. (2008). *Eur. J. Radiol.* **68**, S3–S7.
Suortti, P., Fiedler, S., Bravin, A., Brochard, T., Mattenet, M., Renier, M., Spanne, P., Thomlinson, W., Charvet, A. M., Elleaume, H., Schulze-Briese, C. & Thompson, A. C. (2000). *J. Synchrotron Rad.* **7**, 340–347.
Wysokinski, T. W., Ianowski, J. P., Luan, X., Belev, G., Miller, D., Webb, M. A., Zhu, N. & Chapman, D. (2016). *Phys. Med.* **32**, 1753–1758.
Zhao, Y., Brun, E., Coan, P., Huang, Z., Sztrókay, A., Diemoz, P. C., Liebhardt, S., Mittone, A., Gasilov, S., Miao, J. & Bravin, A. (2012). *Proc. Nat. Acad. Sci. USA*, **109**, 18290–18294.
Zhong, Z., Dilmanian, F. A., Bacarian, T., Zhong, N., Chapman, D., Ren, B., Wu, X. Y. & Weinmann, H. J. (2001). *Med. Phys.* **28**, 1931–1936.
Zhong, Z., Thomlinson, W., Chapman, D. & Sayers, D. (2000). *Nucl. Instrum. Methods Phys. Res. A*, **450**, 556–567.